ELSEVIER

Journal of Fluids and Structures 22 (2006) 197–211

JOURNAL OF FLUIDS AND STRUCTURES

www.elsevier.com/locate/jfs

On shear flow single mode lock-in with both cross-flow and in-line lock-in mechanisms

H. Marcollo[a,*], J.B. Hinwood[b]

[a]AMOG Consulting, 19 Business Park Drive, Notting Hill, 3800, Australia
[b]Department of Mechanical Engineering, Monash University Clayton, 3800, Australia

Received 11 January 2004; accepted 10 October 2005

Abstract

A long flexible cylinder exposed to ocean currents is known to undergo vortex-induced vibration (VIV). In a spatially sheared flow the response of a riser to VIV can vary from single mode lock-in to multimodal. A new experimental facility was designed and built to investigate the above-mentioned areas. The facility consisted of a long flexible cylinder in either a uniform or a simplified vertically sheared flow. The instrumentation consisted of direct local fluid force measurement at two locations on the cylinder as well as accelerometers spaced along the cylinder axis. The simplified shear flow was a 2-slab flow, with each slab having uniform velocity. Test conditions included forcing the cylinder simultaneously at resonance in both regions to investigate modal competition issues and multimodal response patterns. Resonant VIV excitation of two different modes simultaneously, was conducted which revealed single mode lock-in of the higher frequency through an unexpected mechanism. The higher frequency mode's damping region underwent in-line excitation at four times the predicted shedding frequency that provided a power-in effect to support the dominant mode's cross-flow response.

1. Introduction

Long flexible pipelines used in the offshore industry can be subject to vortex-induced vibration (VIV). Drilling and production risers, tension-leg platform tendons, pipeline spans as well as umbilicals are the most affected by VIV which leads to increases in their hydrodynamic loading and reduction in their service life due to fatigue. The most undesirable form of VIV for the offshore industry is termed *lock-in*. Lock-in is used to describe an elastic structure's ability to control the shedding process in a bandwidth around its resonant frequency and for flexible cylinders occurs as single mode, single frequency response. Associated with lock-in is a larger amplitude of excitation increasing unwanted effects. Lock-in always occurs for some velocities in uniform flow conditions; however, in spatially sheared flow conditions the occurrence of lock-in is more complicated. In the ocean, risers are generally exposed to a shear current profile over their depth and hence establishing the boundaries of lock-in and determining the necessary conditions to avoid it is a critical area of research.

*Corresponding author. Tel.: +61 3 95589077.
E-mail address: haydenm@mit.edu (H. Marcollo).

0889-9746/$ - see front matter
doi:10.1016/j.jfluidstructs.2005.10.001

1.1. Response of a structure to VIV

The response of a riser may be described in terms of standing wave modes: modal numbers; mode shapes and modal frequencies (Gopalkrishnan, 1993; Vikestad, 1998). This provides the simplest and most easily applied measure, permitting linear superposition of modes but accounting for nonlinear effects through the inclusion of nonresonant modes. The alternative of using complex modes (Moe et al., 2001) accommodates the effect of phase changes within a mode, due to damping or propagating modes. However, for the length to diameter ratio (L/D) and riser stiffness used here, phase differences along the riser were negligible and the use of complex modes was unnecessary. Thus the parameters describing the response are the peak amplitude or amplitude/diameter (A/D) ratio and the frequency or nondimensional frequency parameter.

VIV response of a lightly damped elastic structure (long elastic structure or rigid spring mounted) varies from in-line response at low reduced velocities (U_r) to cross-flow response at higher U_r. The response depends on a range of structural and fluid flow variables which may be grouped in various ways (Vandiver, 1993; Moe and Wu, 1990). This study has made use of the reduced velocity defined by the still water natural frequency, U_r, and a vibration frequency variable termed the nondimensional frequency ratio, $f_{\text{vib}}/f_{\text{vo}}$. Other informative terms included are the damping ratio, ζ, and the mass ratio, $m^* = \rho_S/\rho_f$. The terms are defined respectively as

$$U_r = U/f_n D, \quad f_{\text{vib}}/f_{\text{vo}} = f_{\text{vib}} D/(\text{St}\, U), \quad \zeta = c/c_r,$$

where U is the fluid velocity, f_n is the still water natural frequency, D is the cylinder diameter, f_{vib} is the measured vibration frequency, f_{vo} is the Strouhal frequency from a stationary cylinder with Strouhal number St, c is the modal damping, c_r is the critical modal damping, ρ_s is the average density of the cylinder, and ρ_f is the density of the fluid.

The present study utilized a nearly neutrally buoyant cylinder in water, and hence a very low mass ratio. For convenience the cylinder used in these experiments will be frequently called a riser. The structural damping was relatively low ($\zeta = 0.04$), as is the case for most long spanning pipelines and risers used offshore.

1.1.1. In-line response

Often the in-line responses of elastically mounted cylinders are neglected in experimental studies of vortex shedding as the cross-flow response amplitude is seen to dominate the total response. However, amplitude is only one variable that determines fatigue damage. Since, the in-line response usually occurs twice at the cross-flow response frequency and twice the mode number, the dynamic curvature can be up to 4 times higher (Huse et al., 2002).

In the absence of cross-flow response, the in-line response of flexible cylinders is reported to occur in the range $1.5 < U_r < 3.5$ (King et al., 1973). The left-hand side of Fig. 1 shows the in-line response of a marine pile model oscillating in water in the flexible cantilever mode as a function of reduced velocity. King performed flow visualization and found the first response region (in Fig. 1) was caused by symmetric vortex shedding, while the second response region was caused by asymmetric vortex shedding. King also found the ratio of in-line vibration frequency to dominant wake frequency slipped into 'convenient' numbers (4:1, 7:2, 3:1, 7:3, 13:6 and 2:1) throughout the in-line lock-in range.

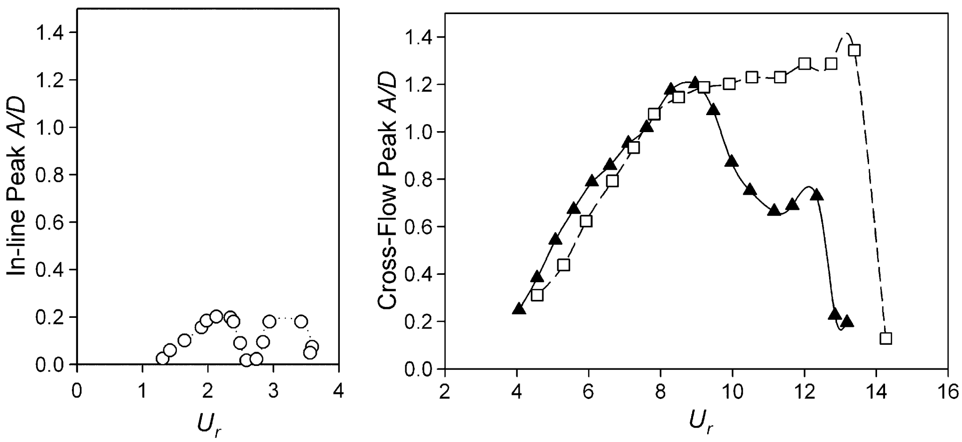

Fig. 1. In-line VIV response of a marine pile model against reduced velocity (King et al., 1973). Typical cross-flow VIV response of elastic structures as a function of reduced velocity (Vandiver, 1993).

Free vibration experiments performed by Moe and Wu (1990) utilized a short rigid cylinder allowed to vibrate in both the in-line and transverse flow directions. The in-line natural frequency in air was set at twice that of the cross-flow natural frequency for the apparatus. Additionally, in a separate experiment, the in-line direction motion was constrained. Moe and Wu found greater cross-flow amplitudes in the free in-line case compared to the constrained in-line case, although the location of peak response differed between the two cases by a factor of 1.5 on the reduced velocity scale. Sarpkaya (1995) and Huse et al. (2002) found similar response trends to Moe and Wu with their short rigid cylinder experiments, although Huse et al. did not present results for the higher levels of reduced velocity as did the other two researchers and hence have not shown the maximum response in the in-line direction that the other two found.

Other studies reported in the literature pertaining to in-line vortex shedding are the following.

In-line vibration frequency of a cantilever has been reported by Pesce and Fujarra (2002). They report the in-line response frequency to jump to four times the natural frequency at values of $U_r > 5$.

Ongoren and Rockwell (1988) performed flow vizualization experiments on short rigid cylinders forced to oscillate in the cross-flow direction, the in-line direction and at angles of 45° and 60° to both. They oscillated the cylinder up to four times the frequency of vortex shedding. Various synchronization patterns were found in the wake at these oscillation frequencies.

Huse et al. (2002) reported the in-line excitation frequency to be four times greater than the cross-flow excitation at low reduced velocities.

1.1.2. Cross-flow response

The right-hand side of Fig. 1 shows the cross-flow response of elastic cylinders as a function of reduced velocity redrawn from Vandiver (1993). The cross-flow response is observed to dramatically increase as U_r increases from 4 to 6. The right-hand side of Fig. 1 also shows the response for two different values of m^* (mass ratio). Typically, as m^* decreases the vibration is more affected by the fluid forces, and the added mass then causes a larger bandwidth of response.

Using true reduced velocity (defined with the actual measured vibration frequency instead of a fixed frequency) as the abscissa, when plotting the VIV response of a structure, removes the effect of mass ratio and added mass. The nondimensional frequency ratio also accomplishes the same result as it uses the actual vibration frequency. The nondimensional frequency ratio, $f_{\mathrm{vib}}/f_{\mathrm{vo}}$ has the advantage that it is normalized with the Strouhal frequency and one can understand what the response is doing in comparison to the shedding frequency. When expressing a lock-in range or power-in bandwidth in terms of $f_{\mathrm{vib}}/f_{\mathrm{vo}}$, the effect of added mass is removed and the ability of the wake to synchronize with the cylinder motion is the only remaining effect.

1.2. Presently used VIV prediction techniques

The most widely industry-accepted VIV prediction tools are empirically based computer programs that predict cross-flow response on the basis of individual modes. For a certain reduced velocity bandwidth of a given mode, the structure is deemed to be excited by the fluid, while all other values of U_r contribute to damping of that modal response. The bandwidth of U_r for excitation can be nominally varied, but will always be in the range $U_r > 4$. Various forms of damping models are applied to the slower and higher reduced velocity regions to estimate modal response.

The VIV of a cylinder may be modelled from fundamental equations or using empirical data, and in the frequency domain or the time domain. Models based on fundamental equations use the methods of computational fluid dynamics to determine the fluid motions and pressures, and hence to determine the hydrodynamic forces acting on the cylinder. Such models need to be coupled to a structural model which computes structural displacements and hence the new fluid boundary conditions. All such models developed operate in the time domain and their use has been limited to research, although in future these models are expected to become the dominant type for major design studies.

The present industry standard models for predicting VIV response of risers or pipeline spans are frequency-domain models using simple displacement modes. Like all frequency-domain models they are inherently linear but the superposition of modes allows for nonlinear processes, in particular the quadratic drag and lift force terms. The analyses carried out in using the present industry standard models makes use of experimentally derived rules to determine whether the response is single or multimodal, and superposes modes in the latter case. Power-in regions for the riser are estimated, and regions outside the assumed power-in length are considered to be damping regions.

The above-mentioned models all use an empirical database for the excitation that relies on previous experimental results to determine lift coefficient (C_L) as a function of U_r and A/D, for example the results of Gopalkrishnan (1993).

Limitations of the models are the assumptions that: (i) modes are considered separately; (ii) in-line modes are of minor importance; and (iii) segments of the cylinder outside a narrow power-in length (bandwidth of U_r values) dissipate VIV energy by hydrodynamic damping. While plausible, there is evidence to show that these assumptions are not correct and it is not known if their use leads to acceptable solutions in all practical cases. The validity of these assumptions are examined in the present paper.

2. Experimental program

2.1. 2-Slab flow facility

The Monash University large wave flume was used for the experiments. The depth of the flume is 4 m. Two large recirculating pumps combine to give a maximum capacity of 850 L/s. The width of the tank was constricted to 320 mm over a 5 m length for the purpose of these experiments to provide velocities high enough to excite the first two cross-flow modes.

A schematic of the facility is shown in Fig. 2 and the apparatus and experimental procedure are described more fully in Marcollo and Hinwood (2002). It comprises a long flexible cylinder mounted in a current. By the use of a thin upstream splitter, terminating $2D$ upstream of the test cylinder, the flow may be divided into two zones, each with its own uniform velocity. The boundary between the zones was kept thin compared with the zone thickness and a check was made on likely interference arising from the large gradient of flow at the interface of the two zones. The disturbance frequencies were much lower than the VIV frequencies of interest.

2.2. Test cylinder and flow conditions

The physical properties of the cylindrical flexible riser model used for the experiments are presented in Table 1.

The model riser was instrumented with four accelerometers, each two axis, and 2 pressure tapping rings to measure response and forcing. The accelerometers were located at $L/6$, $L/4$, $L/2$, and $3L/4$, where L is the length of the riser. The axial locations of the pressure tapping rings were as close to $L/4$ and $3L/4$ as possible (each was 50 mm in the axial direction towards the centre of the riser model, respectively). Each of the pressure tapping rings forms a 6-point

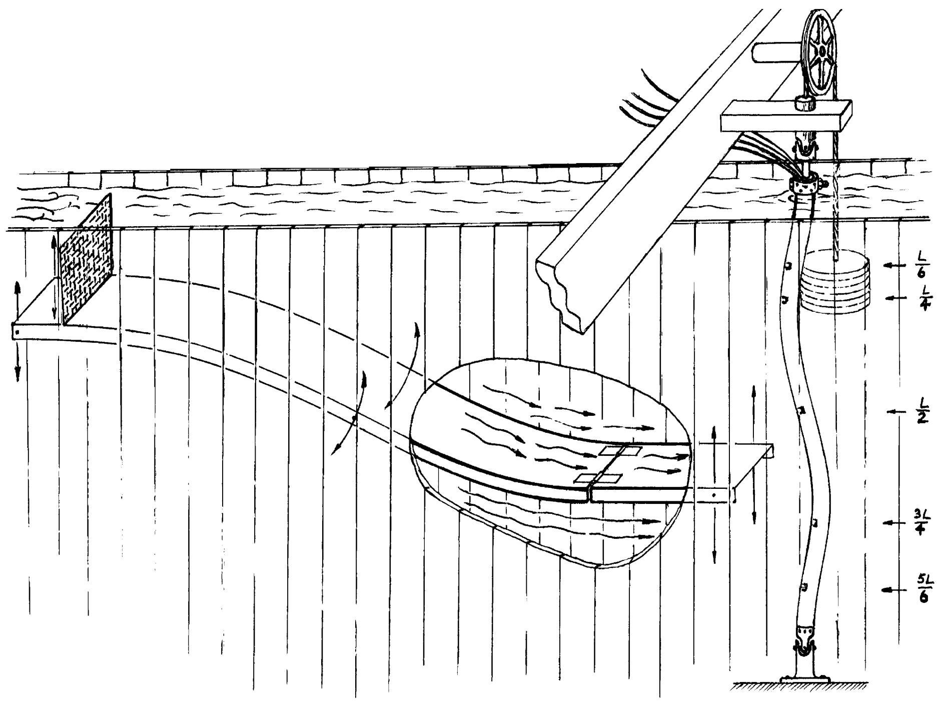

Fig. 2. A sketch of the experimental setup (Marcollo and Hinwood, 2002).

Table 1
The physical properties of the model

Bending stiffness (EI)	$74\,\mathrm{N\,m^2}$
Length (L)	3.58 m
Mass per unit length ($\rho_s L$)	1.28 kg/m
Outside diameter (D)	40 mm
Aspect ratio (L/D)	90
End conditions	Pin-pin

pressure tapping system to derive the local lift force. A small dynamic correction had to be made to correct for fluid inertial effects between the pressure sensing membrane and the outer surface of the riser model.

Reduced velocity could be varied either through the velocity of flow or the value of end tension which alters the natural frequency. Plots of the systematic variation in reduced velocity given in this paper always originate from the flow velocity being varied. The number of velocity increments tested varied, but always exceeded ten.

Three different power-in lengths were selected based on the limits of the facility to be able to generate uniform flow within each section of the flow. The power-in lengths were defined as the percentage of the model length exposed to higher speed flow to the total length. The power-in lengths reported are 30%, 35% and 40%. The uniformity of flow within each slab was lost for power-in lengths above and below these values. Only the results for the 30% power-in length are reported here.

The turbulence intensity was always in the range 5–10%, generally with a macro length scale, $L_u = 100\,\mathrm{mm}$. Reynolds number varied from 8×10^3 to 4×10^4.

2.3. Modal participation factors

The accelerometer time signals were post-processed together to determine modal participation factor time series. Firstly, the accelerometer signal was converted to a displacement time series by Fourier transforming, dividing each Fourier component by the frequency value squared of the abscissa and then inverse Fourier transforming. All signals were high-pass filtered in post-processing at 0.9 Hz to prevent 'blow-up' that commonly occurs due to low frequency noise when converting acceleration to displacement. Once the displacement time series was obtained, the modal participation time series $q_i(t)$, for mode i, was determined by assuming that the various displacements at a given time consist of the sum of the first four orthogonal modes (each operating harmonically). The time series of the amplitude for each individual mode shape (modal participation factor), $q_i(t)$, was then back calculated from

$$y(z,t) = \sum_{i}^{n} \phi_i(z) q_i(t), \tag{1}$$

where $y(z,t)$ is the displacement of the riser at height z, and $\phi_i(z)$ is the mode shape factor for mode i. In the context of this paper the mode shapes are assumed of sinusoidal form and defined as

$$\phi_i(z) = \sin\left(\frac{i\pi z}{L}\right). \tag{2}$$

It has been shown that the natural modes of a structure in shear flow differ from those in still water (Triantafyllou, 1998). In Triantafyllou (1998) the natural modes of the coupled fluid/structure system were numerically solved for by iterating with previously found coefficients from towing tank testing. Without a numerical solver we instead do a check on the natural modes for two resonant conditions in shear flow and determine their shape. For the resonant condition of Mode 1 in shear flow it is found that the displacement participation factors for the natural measured modeshape, when compared to a pure Mode 1 sinusoid, sum to an error of 12%. For the resonant condition of Mode 2 in shear flow it is found that the displacement participation factors, when compared to a pure Mode 2 sinusoid, sum to an error of 15%. The reason for the natural modeshapes' departure from sinusoid in a shear flow is due to the spatially varied added mass. The unknown variability of added mass and hence the unknown modeshapes when different regions of a riser are strongly interacting with each other, as in nonresonant conditions, leads us to the use of sinusoids for the estimation of modal participation factors in the analyses of the following sections.

3. Results

3.1. Amplitude

Fig. 3 shows a typical velocity profile on the left-hand side. The 2-slab flow was designed so that the bottom layer would excite Mode 2 cross-flow and the top layer would be simultaneously attempting to excite Mode 1 cross-flow. Both of these velocities were systematically varied together and the resulting modal participation response of each mode is shown on the right-hand side of Fig. 3. The plots on the right-hand side are shown against their respective reduced velocity based on the natural frequency in still water of the respective mode.

The response in Fig. 3 shows the unexpected results that Modes 1 and 2 do not equally gain in response amplitude at their ideal lock-in range of reduced velocity where the largest excitation is reached. Instead, when $U_r \approx 8$, Mode 2 takes over the whole riser system and dominates the response, while Mode 1 significantly decreases in response. This is a clear example of a breakdown in the premise of considering each mode separately in estimating its likely response amplitude. It is obvious that the response of Mode 1 cannot be predicted on its own.

The cross-flow time series and spectra of various conditions in which both Modes 1 and 2 were excited are shown in Fig. 4.

The narrow band responses in Fig. 4 are characteristic of a resonant response and show that the cross-flow response frequency occurs at around the natural frequency. It shows clearly how, at location 'B', Mode 2 is dominating the response. For the highest velocity condition shown, 'C', the response in Mode 1 is observed to increase again.

A more detailed picture of the response displacement amplitude is shown in Fig. 5. The components of cross-flow (C.F.) response are shown for Modes 1 and 2, Fig. 5; the in-line (I.L.) components are also shown up to Mode 3. Above these mode numbers, the response is almost insignificant and thus not shown.

It can be observed in Fig. 5 that at the point where C.F. Mode 1 response dramatically decreases (the vertical dashed line) as a function of U_r, both the C.F. Mode 2 and the I.L. Mode 3 responses significantly increase. The unexpected result of Mode 2 dominating the response (where Mode 1 response declines) is subject to further investigation later in this paper.

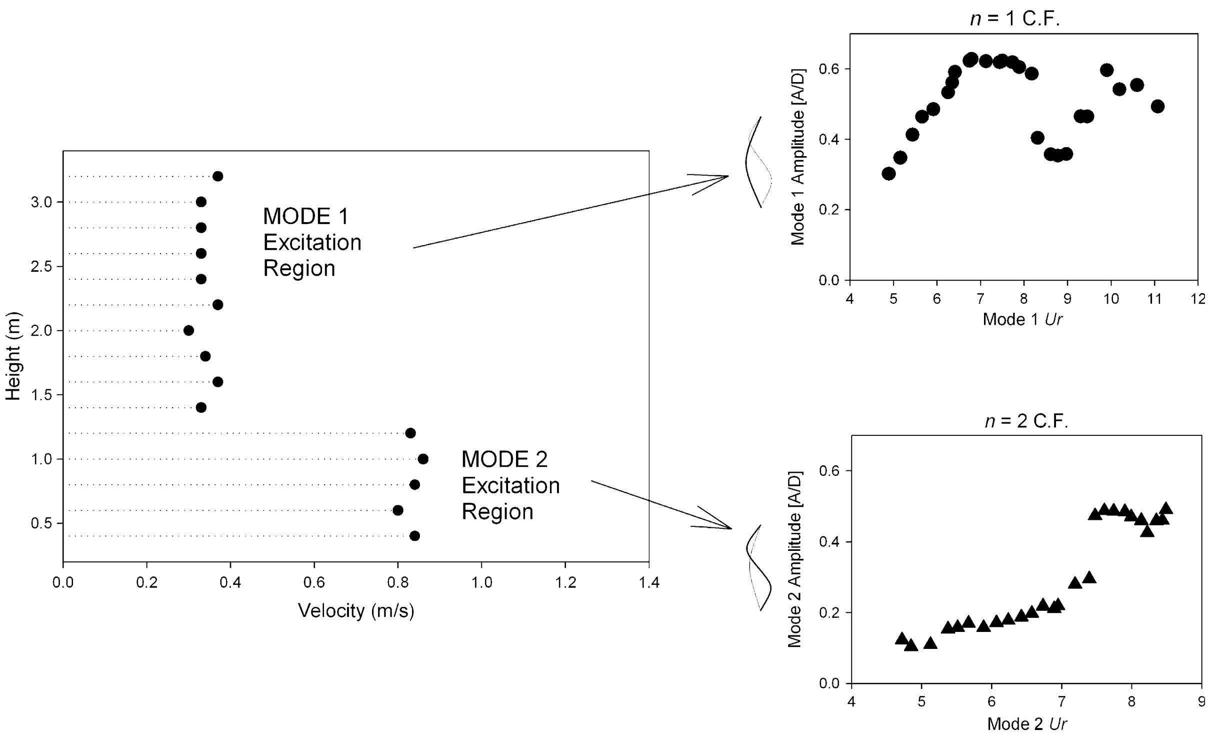

Fig. 3. A typical 2-slab flow profile on the left for a given test. On the right, the respective Modes 1 and 2 contributions to overall response for each test as a function of their respective reduced velocity.

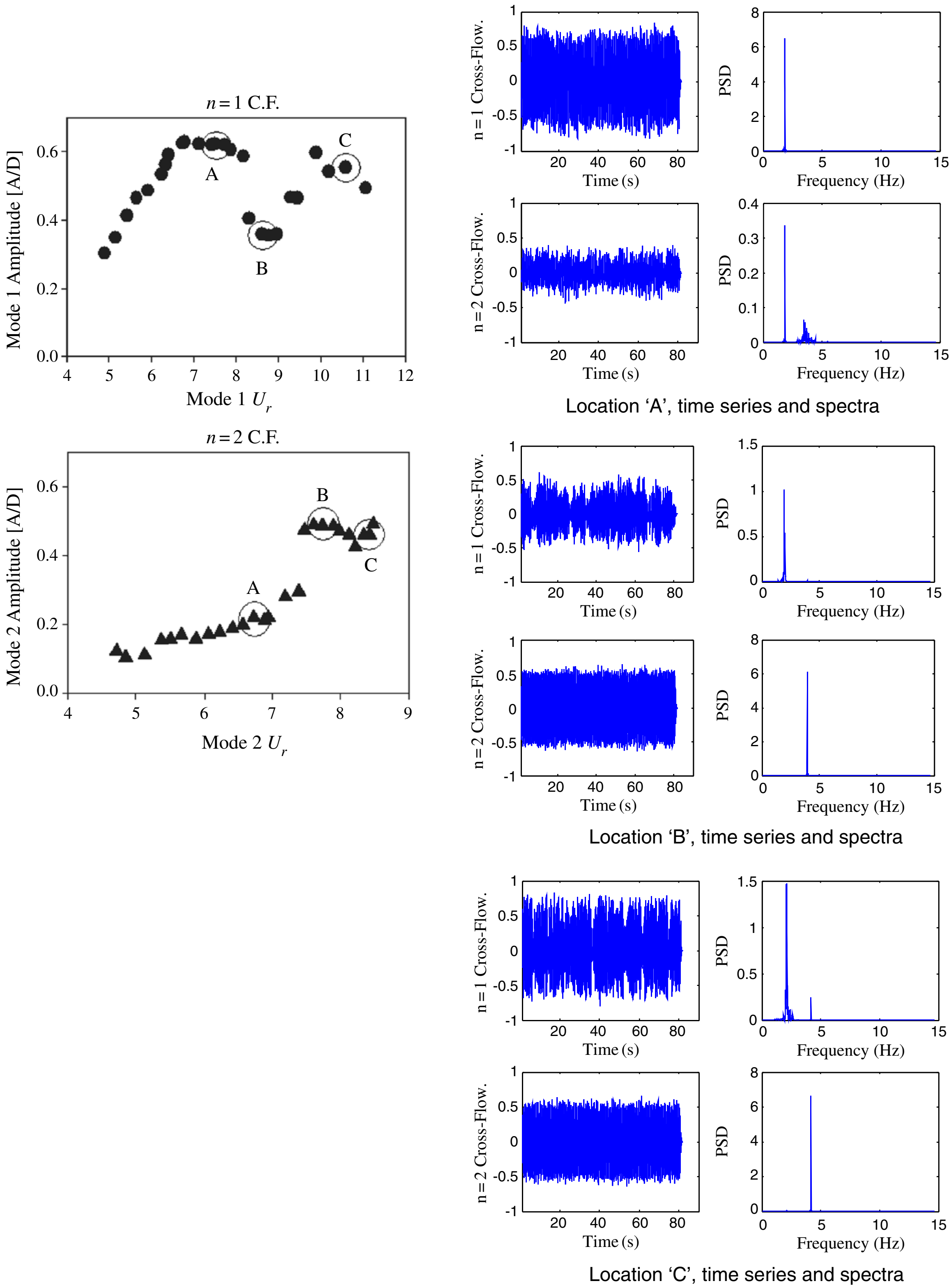

Fig. 4. Time series and spectra of the modal participation series for Modes 1 and 2 at the simultaneous conditions shown on the LHS graph.

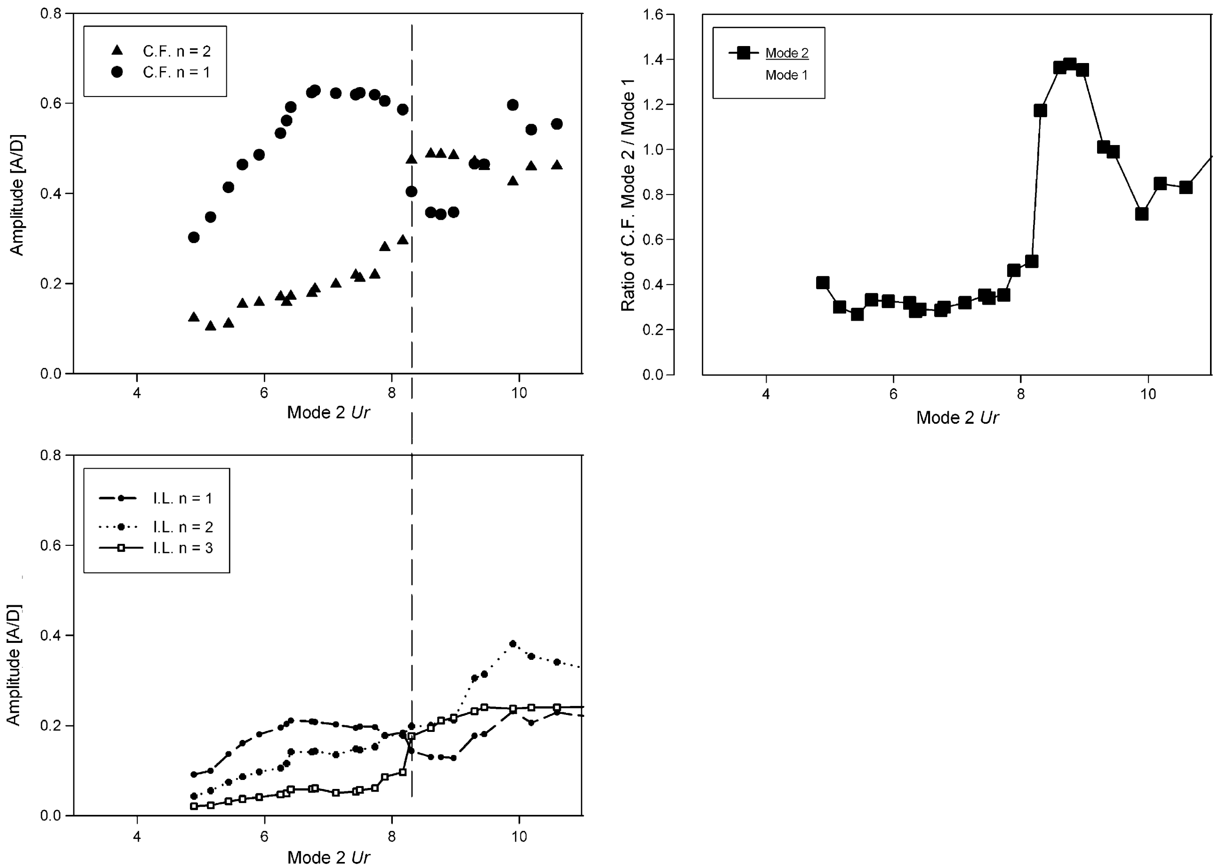

Fig. 5. Cross-flow (C.F.) and in-line (I.L.) components of response as a function of bottom layer velocity (Mode 2 U_r). The vertical dashed line shows the value of reduced velocity where the simultaneous dramatic change in cross-flow response occurs.

From Fig. 5 the following general observations can be made, despite some irregularities in the curves:

(a) Mode 1 is observed to dominate the response for reduced velocities less than the simultaneous resonant condition ($U_r < 7$);
(b) the amplitude of Mode 2 response increases as a function of U_r in the range $7 < U_r < 8$, while simultaneously Mode 1 response decreases;
(c) the ratio of Mode 2 to Mode 1 provides an estimate of the dominance of Mode 2 in the response.

3.1.1. Kurtosis of displacements

The kurtosis of the displacements is an empirical criterion that has previously been used to classify response into either a multimode ($K \sim 3$) mixture or single mode lock-in ($K \sim 1.5$) (Vandiver, 2000). Kurtosis is defined as

$$K = \frac{\langle q_i^4 \rangle}{\langle q_i^2 \rangle^2}, \tag{3}$$

where $\langle\,\rangle$ represents the mean. The kurtosis is evaluated on the present data for Mode 1 displacement participation factors and Mode 2 displacement participation factors and is shown in Fig. 6. The Mode 2 kurtosis falls to the lock-in value of 1.5 at the same value of U_r that the Mode 2 amplitude begins to dominate the response; whereas Mode 1 exhibits a lock-in type response in the range $4.5 < U_r < 7.5$ (lower than the Mode 2 dominance region). When examined in conjunction with the amplitude response, the kurtosis appears to be a successful classification tool in this case.

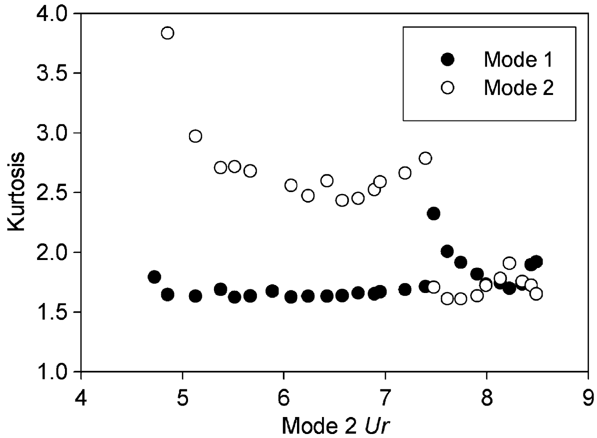

Fig. 6. Kurtosis of Modes 1 and 2 C.F. amplitude responses as a function of Mode 2 reduced velocity.

3.2. Lift coefficient

The single degree of freedom equation of motion can be used to model the modal response of a structure subjected to VIV:

$$m\ddot{y} + c\dot{y} + ky = F_o \cos \varphi \sin \omega t + F_o \sin \varphi \cos \omega t, \tag{4}$$

where y is the displacement and $F_o \sin(\omega t - \phi)$ is the forcing function.

The lift coefficient is defined as

$$C_L = \frac{F_o}{\frac{1}{2}\rho DLU^2}. \tag{5}$$

Power flow from the fluid to the cylinder can be expressed in terms of the lift coefficient in phase with the velocity:

$$\overline{P} = \tfrac{1}{4}\omega y_o \rho LDU^2 C_{L_V}. \tag{6}$$

Measurements of the lift force time series were decomposed into components in phase with local riser velocity and in phase with local riser acceleration and from these series the lift coefficient in phase with the velocity,

$$C_{L_V} = C_L \sin \varphi, \tag{7}$$

was obtained.

The lift coefficient, C_{L_V}, is shown in Fig. 7 from the pressure tapping rings in each of the slower and faster regions as a function of reduced velocity. Also included in Fig. 7 is the location of sudden riser response change in the form of a vertical dashed line.

The values of C_{L_V} in the plots of Fig. 7 were created using the local cross-flow riser velocity which consists of the sum of the first two modes of response. Each flow region has a unique interaction with each mode of response of the riser. By examining the modal responses (from Fig. 5) in tandem with values of C_{L_V} (in Fig. 7) one can see a sudden jump in C_{L_V} occurs in the slower flow region at the same time that Mode 1 decreases and Mode 2 dominates the response. The positive values of C_{L_V} in the slower region indicates that power is being transferred from the fluid to the structure and, as Mode 2 largely dominates in this range of U_r values, this indicates that Mode 2 is being excited in the slower flow region as well as the faster flow region.

3.3. Slow flow region

In order to examine further what is happening between the riser and the fluid in the slow flow region, the amplitude and frequency of response are presented for all the different responses of the riser in Fig. 8. Frequency of response is best presented in terms of a parameter that has been nondimensionalized with respect to the slower region's expected

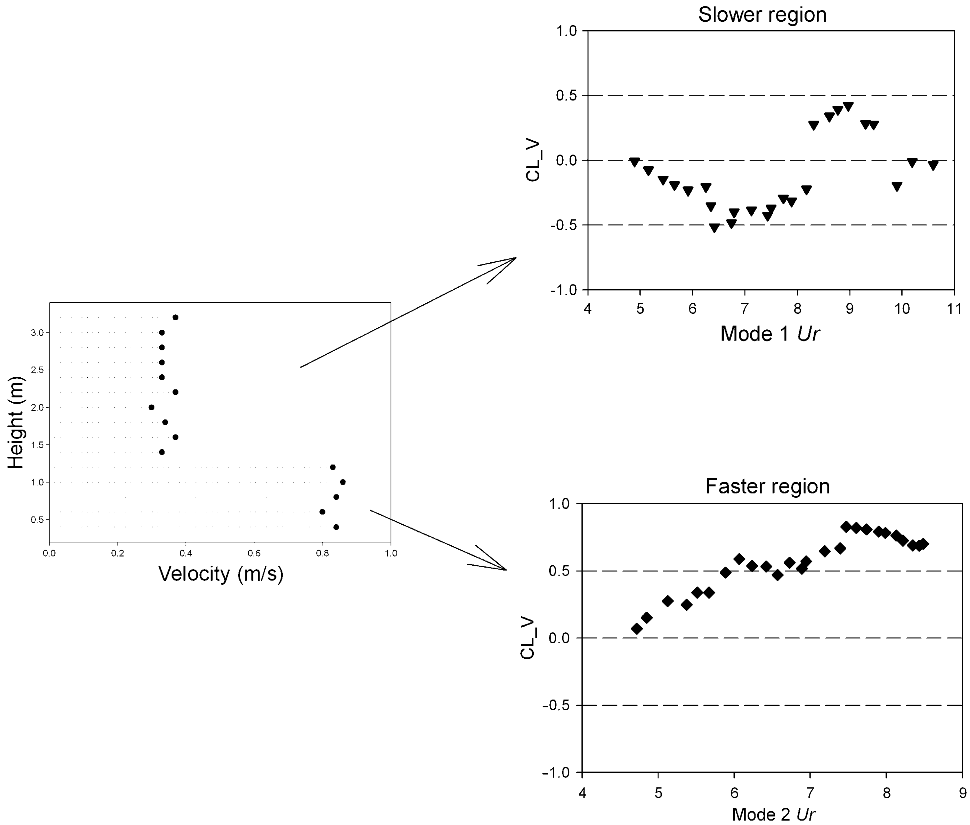

Fig. 7. Lift coefficient in phase with cylinder velocity from the faster and slower regions as a function of reduced velocity.

vortex shedding frequency, using $\mathrm{St} = 0.15$. The vibration frequency of response is then presented as a nondimensionalized value.

The nondimensional frequency ratio for in-line Mode 3 is shown in Fig. 8 to vary the most of all the modes, peaking at a value of 4.0. This means that the riser is vibrating in-line at four times the predicted shedding frequency. The other in-line modes have frequency ratios in the vicinity of 2.0, which is approximately what one would expect for the in-line excitation frequency; it would be twice the shedding frequency.

The strong increase in amplitude of Mode 3 in-line, while simultaneously Mode 2 cross-flow dominates the response, indicates Mode 3 *in-line* may be the reason for Mode 2 cross-flow dominance. The unique value of $f_{\mathrm{vib}}/f_{\mathrm{vo}} = 4.0$ for Mode 3 in-line, that matches previously measured excited values from other research reviewed in the literature (Section 2) builds the case that Mode 3 in-line causes Mode 2 cross-flow to dominate.

3.4. Cross-correlation analyses

For final confirmation that Mode 3 in-line causes the Mode 2 dominant lock-in effect, a cross-correlation analysis was performed. The analysis was conducted on all the in-line and cross-flow modal participation factors with the exciting cross-flow fluid force in the slower region. The fluid force exhibits two clear peaks in its spectra, one at Mode 1 response frequency, and one at Mode 2 response frequency. The fluid force was filtered prior to conducting the correlation and the component of fluid force at the Mode 2 frequency was used in the correlation. A peak cross-correlation coefficient was calculated as

$$\rho_{xy} = \max\left\{ \frac{C_{xy}(\tau)}{\sqrt{C_{xx}(0)C_{yy}(0)}} \right\}, \tag{8}$$

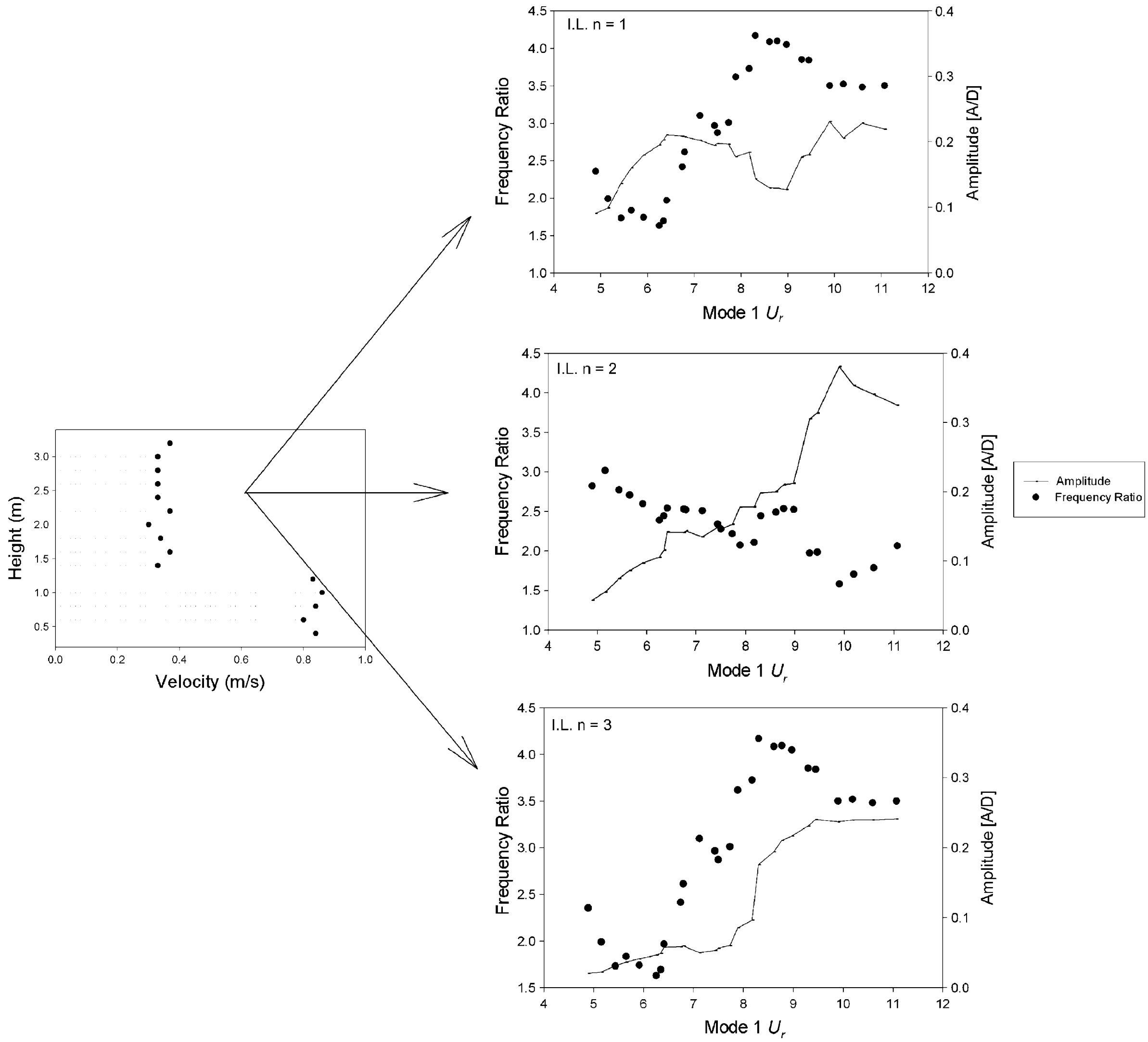

Fig. 8. The first three in-line response modes of the riser. Amplitudes and nondimensional frequency ratios as functions of reduced velocity for the slower layer.

where ρ_{xy} is the peak of the cross-correlation, C_{xy}, is the maximum value across the range of τ. Fig. 9 shows ρ_{xy} for Mode 3 in-line. Also shown is the actual vibration frequency and a dotted line showing where the vibration frequency equals four times the shedding frequency.

Fig. 9 shows ρ_{xy} for Mode 3 in-line peaks at 0.8 at exactly the same location as the in-line vibration frequency is approximately four times the expected shedding frequency. As an indication of just how strong the previous correlation is, the next largest correlation between *any* mode and *any* fluid forcing was 0.5 (all combinations were tried although not shown graphically). Shown in the graph is the range where the correlation is high, indicating that the fluid pressure distribution is very highly correlated to the motion and thus there is a dominant 'wake capture' effect, also corresponding to four times the shedding frequency.

In summary, in the current section it has been shown that the supposed Mode 1 power-in region actually helps the Mode 2 peak (for a narrow range of reduced velocity) by an in-line lock-in (Mode 3) effect.

It is not known exactly why the coupled fluid/structure system in the slower flow region does not maintain the preferred Mode 1 cross-flow response and decides to switch from the Mode 1 natural frequency cross-flow response and

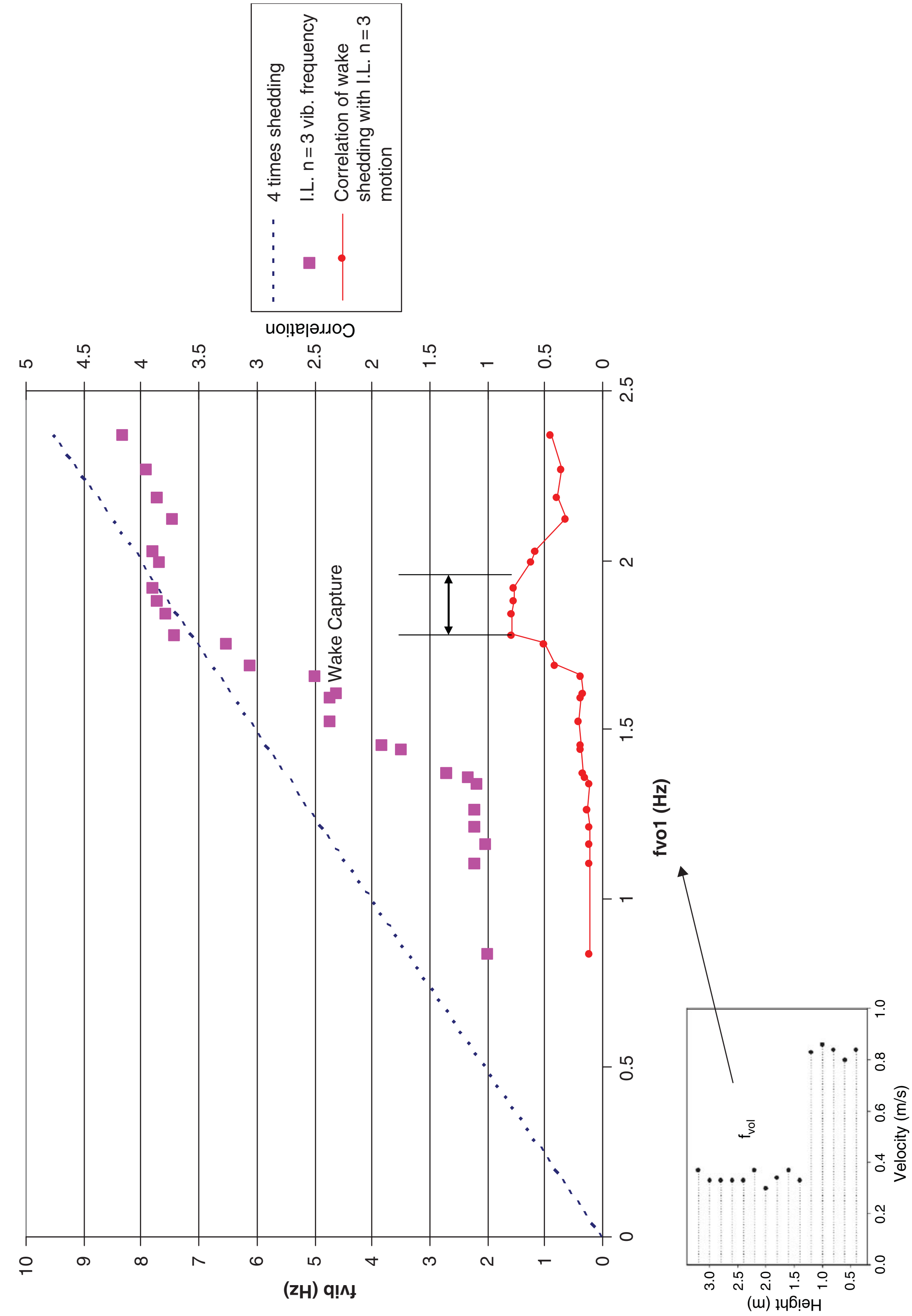

Fig. 9. Correlation of wake shedding with Mode 3 in-line motion.

choose an in-line lock-in response mode that supports Mode 2 cross-flow. Flow visualization of fluid-structure interaction in the slower flow region would be a valuable next step in unraveling the mysteries of the in-line lock-in effect.

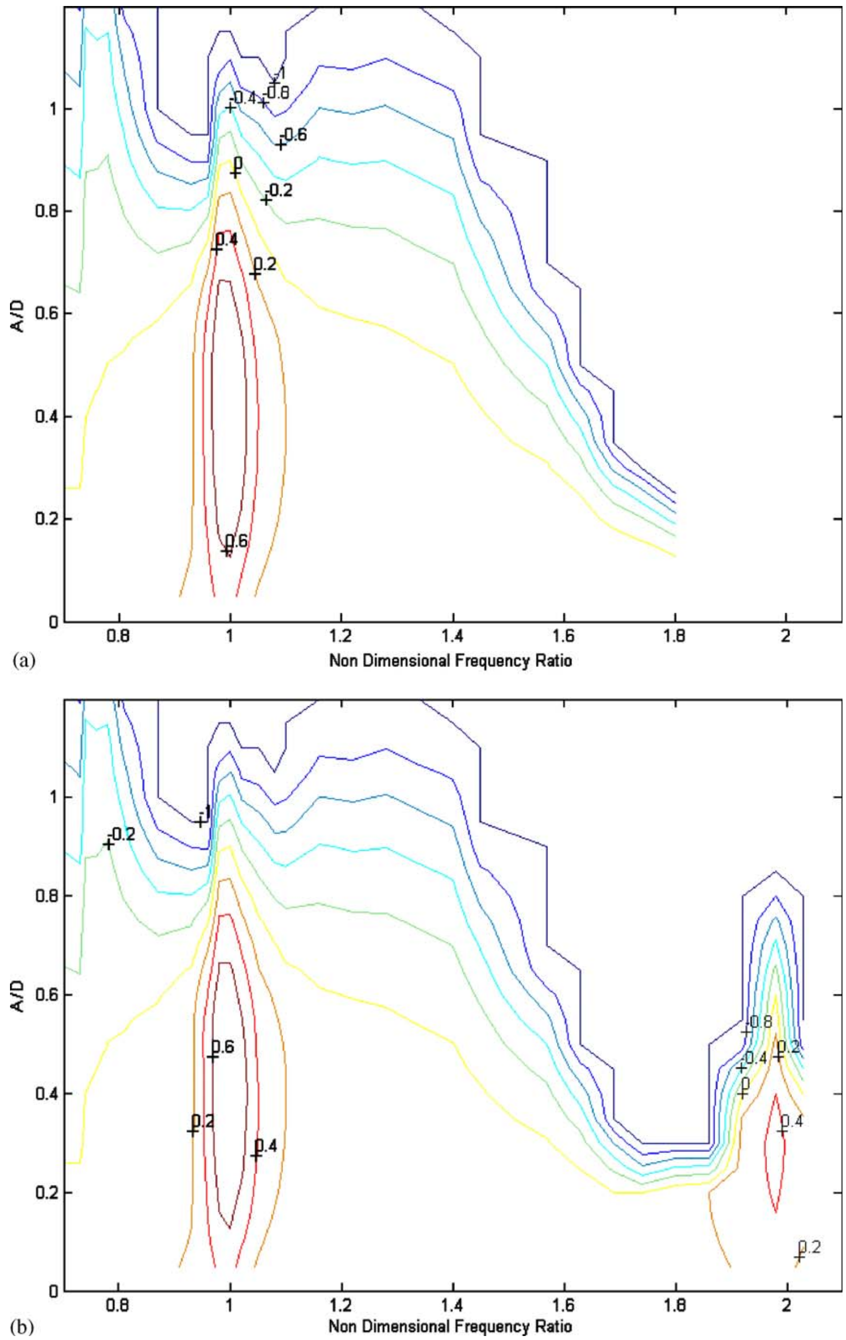

Fig. 10. (a) Approximation of Gopalkrishnan's original data. (b) Modified data to take into account in-line excitation in the cross-flow shear model.

4. Implementation in semi-empirical prediction methods

One way of modelling the slow flow region effect is to assume that excitation (through the in-line direction) occurs at high f_{vib}/f_{vo} (or low U_r) and model some power-in from this range that would support the cross-flow response.

Implementation in current VIV prediction models is preformed by increasing the lift coefficient value at high (or low U_r). If the in-line response occurs at $f_{vib}/f_{vo} = 4.0$, then the equivalent cross-flow response value would be $f_{vib}/f_{vo} = 2.0$ (as in-line response is generally twice the frequency of cross-flow). Fig. 10(a) shows an approximation to Gopalkrishnan's lift coefficient data that is commonly implemented for VIV prediction of bare risers. Fig. 10(b) shows a modification to Gopalkrishnan's data with an increased lift coefficient region at high f_{vib}/f_{vo}. The modified C_L data was created by trial and error with a semi-empirical prediction tool until the predicted response trend from the tool matched the experimentally observed response trend.

5. Conclusions

The motions of an elastic cylinder of intermediate length capable of being excited in several modes of vibration may be well described by the superposition of simple harmonic modes. The motion of the cylinder in a sheared flow may display single or multi-mode behavior depending on the power input to each of the competing modes. Direct fluid force measurements provide an indication of the direction of power transfer and can show exactly how a region contributes to the riser response.

In-line motion is shown to be of vital importance in predicting single mode cross-flow lock-in events in a simplified shear flow. In a shear flow an in-line VIV can occur at low U_r (as in uniform flow tests), dominating over lower frequency cross-flow response alternatives and supporting another region's higher frequency cross-flow resonant response. Through this mechanism the apparently nonresonant region of a riser can contribute to the excitation, whereas this region has been previously regarded as being a damping region.

A modified C_L contour map can be applied to the latest empirically based VIV cross-flow prediction programs to model the increased propensity for power flow into a cross-flow mode via slower flow region in-line lock-in.

Acknowledgements

The current publication is a result of the first author's doctoral dissertation conducted at the Department of Mechanical Engineering, Monash University. The first author was provided with financial support from an APA (Australian Postgraduate Award).

Professor J.K. Vandiver of the Department of Ocean Engineering, MIT was involved at the initial stages with the conceptual design of the experiment.

References

Gopalkrishnan, R., 1993. Vortex-induced forces on oscillating bluff cylinders, Ph.D. Thesis, MIT, Cambridge, MA, USA.

Huse, E, Nielsen, F.G., Soreide, T., 2002. Coupling between in-line and transverse VIV response. In: Proceedings of the 21st International Conference on Offshore and Arctic Mechanics, June 2002, Oslo, Norway, paper OAME2002-28618.

King, R., Prosser, M.J., Johns, D.J., 1973. On vortex excitation of model piles in water. Journal of Sound and Vibration 29, 169–188.

Marcollo, H., Hinwood, J.B., 2002. A facility for the evaluation of modal competition in an elastic riser. In: Proceedings of ISOPE, 2002, vol. 2. Kita-Kyushu, Japan, p. 55.

Moe, G., Wu, Z.-J., 1990. The lift force on a cylinder vibrating in a current. ASME Journal of Offshore Mechanics and Arctic Engineering 112, 297–303.

Moe, G., Arntsen, O., Hoen, C., 2001. VIV analysis of risers by complex modes. In: Proceedings of ISOPE 2000, vol. 3, pp. 426–430.

Ongoren, A., Rockwell, D., 1988. Flow structure from an oscillating cylinder Part 2. Mode competition in the near wake. Journal of Fluid Mechanics 191, 225–245.

Pesce, C.P., Fujarra, A.L.C., 2002. Vortex induced vibrations experiments with an elastically mounted cylinder in water. In: Proceedings of ISOPE, 2002 Japan, pp. 502–509.

Sarpkaya, T., 1995. Hydrodynamic damping, flow-induced oscillations, and bi-harmonic response. ASME Journal of Offshore Mechanics and Arctic Engineering 117, 232–238.

Triantafyllou, G.S., 1998. Vortex induced vibrations of long cylindrical structures. In: Proceedings of the ASME Summer Meeting, vol. 50, Washington, DC, pp. 1–8.

Vandiver, J.K., 1993. Dimensionless parameters important to the prediction of vortex-induced vibration of long, flexible cylinders in ocean currents. Journal of Fluids and Structures 7, 423–455.

Vandiver, J.K., 2000. Predicting lock-in on drilling risers is sheared flows. In: Proceedings of the Flow-Induced Vibration 2000 Conference, Lucerne, Switzerland.

Vikestad, K., 1998. Multi-frequency response of a cylinder subjected to vortex shedding and support motions. Dr. ing. Thesis. Department of Marine Structures, Norwegian University of Science and Technology, Trondheim, Norway.